

**A reproducible effect size is more useful  
than an irreproducible hypothesis test to  
analyze high throughput sequencing  
datasets**

**Andrew D. Fernandes<sup>1</sup>, Michael Vu<sup>2</sup>, Lisa-Monique Edward<sup>3</sup>, Jean M.  
Macklaim<sup>4</sup>, and Gregory B. Gloor<sup>5</sup>**

<sup>1</sup>San Diego CA, 92130

<sup>2</sup>Department of Biochemistry, University of Western Ontario, London, N6A 5C1, Canada

<sup>3</sup>Department of Biochemistry, University of Western Ontario, London, N6A 5C1, Canada

<sup>4</sup>DNA Genotek, Ottawa, K2V 1C2, Canada

<sup>5</sup>Department of Biochemistry, University of Western Ontario, London, N6A 5C1, Canada

Corresponding author:

G. Gloor<sup>5</sup>

Email address: ggloor@uwo.ca

**ABSTRACT**

16 High throughput sequencing is analyzed using a combination of null hypothesis significance testing and  
17 ad-hoc cutoffs. This framework is strongly affected by sample size, and is known to be irreproducible  
18 in underpowered studies, yet no suitable non-parameteric alternative has been proposed. Here  
19 we present implementations of non-parametric standardized median effect size estimates,  $\mathbb{E}$ , for  
20 high-throughput sequencing datasets. Case studies are shown for modelled data, transcriptome and  
21 amplicon-sequencing datasets. The  $\mathbb{E}$  statistic is shown to be more reproducible and robust than p-values  
22 and requires sample sizes as small as 5 to reproducibly identify differentially abundant features. Source  
23 code and binaries freely available at: <https://bioconductor.org/packages/ALDEx2.html>, [omicplotR](#), and  
24 <https://github.com/ggloor/CoDaSeq>. Datasets can be found at doi://10.6084/m9.figshare.8132216  
25

## 26 INTRODUCTION

27 High throughput sequencing (HTS) datasets for transcriptomics, metagenomics and 16S rRNA gene  
28 sequencing are high dimensional and generally conducted at pilot-scale sample sizes. Much effort has  
29 been spent identifying the best approaches and tools to determine what is ‘significantly different’ between  
30 groups (Soneson and Delorenzi, 2013; Schurch *et al.*, 2016), but the answer seems to depend on the  
31 specific dataset and associated model parameters (Thorsen *et al.*, 2016; Hawinkel *et al.*, 2018; Weiss *et al.*,  
32 2017). As commonly conducted the investigator determines what is ‘significantly different’ using a null  
33 hypothesis significance approach and then decides what level of difference is ‘biologically meaningful’  
34 among the significantly different features. Graphically, this approach is represented by the Volcano plot  
35 (Cui and Churchill, 2003) where the magnitude of change (difference) is plotted vs the p-value. One  
36 under-appreciated consequence of pilot scale research is that features with significant p-values will often  
37 have dramatically exaggerated apparent effect sizes and consequently very low apparent p-values (Halsey  
38 *et al.*, 2015). This explains in part why so many observations of apparent large effect fail to replicate  
39 in larger datasets (Ioannidis, 2005). In fact, both p-values and absolute difference are poor predictors  
40 of replication likelihood if the experiment were conducted again (Cumming, 2008; Halsey *et al.*, 2015).  
41 Null-hypothesis significance based testing methods also have the property that the number of significant  
42 features identified is affected by the number of samples being compared. This leads to the concept of

43 statistical power which often is prioritized over biological significance.

44 On the other hand, a standardized effect size addresses the issues of interest to the biologist: “what is  
45 reproducibly different?” or “would I identify the same true positive features as differential if the experiment  
46 were repeated?” (Coe, 2002; Nakagawa, 2004; Colquhoun, 2014; Gloor *et al.*, 2016b). Standardized effect  
47 size statistics start from the assumption that there is a difference, but that the difference can be arbitrarily  
48 close to zero. Unfortunately, standardized effect size metrics are not routinely used when analyzing HTS  
49 datasets, and one potential barrier is that parametric effect size statistics may not be suitable for HTS  
50 datasets because the data cannot often be assumed to fit a Gaussian distribution.

The most widely used standardized effect size is Cohen’s  $d$ , which is a parametric standardized effect size for the difference between the means of two groups. The general formulation is given in Equation 1,

$$\text{Cohen's } d = \frac{\text{mean}(a) - \text{mean}(b)}{\sigma_{a,b}} \quad (1)$$

51 and is essentially a Z score. Cohen’s  $d$  measures the difference between the means of the two distributions  
52 divided by the pooled standard deviation, denoted as  $\sigma_{a,b}$ . However, this metric depends upon the data  
53 being relatively Normal, which cannot be guaranteed for HTS data as seen in Figure 1.

54 The purpose of this report is to show that we can characterize the difference between distributions in a  
55 non-parametric manner without resorting to a rank-based approach that discards much information. We  
56 introduce a simple non-parametric standardized effect size statistic for distributions,  $\mathbb{E}$ , that is calculated  
57 as the median effect size for the differences of the distributions. This measure is implemented in the  
58 ALDEx2, omicplotR and CoDaSeq R packages. The  $\mathbb{E}$  statistic has been used in both meta-transcriptome  
59 and microbiome studies, for example see (Macklaim *et al.*, 2013; Bian *et al.*, 2017), and has been shown  
60 to give remarkably reproducible results even with extremely small sample sizes (Nelson *et al.*, 2015).  $\mathbb{E}$   
61 has a near monotonic relationship with p-values, but is stable between sample sizes (Supplement Figure  
62 1). However, it is unknown how  $\mathbb{E}$  compares with parametric effect size estimates, how many samples are  
63 required, and its sensitivity and specificity characteristics.

## 64 METHODS

### 65 Calculating $\mathbb{E}$

66 High throughput sequencing (HTS) machines output thousands to billions of ‘reads’, short nucleotide  
67 sequences that are derived from a DNA or RNA molecule in the sequencing ‘library’. The library is a  
68 subset of the nucleic acid molecules that have been collected from an environment and made compatible  
69 with a particular HTS platform. The HTS instruments deliver these reads as integer ‘counts’ per genomic  
70 feature—gene, location, etc (?). However, the counts are actually a single proxy for the probability of  
71 observing the particular read in a sample under a repeated sampling model; this is clear since technical  
72 replicates of the same library return different counts. The difference between technical replicates is  
73 consistent with multivariate Poisson sampling (Fernandes *et al.*, 2013; Gloor *et al.*, 2016a) The probability  
74 estimate is delivered by the instrument as an integer representation of the probability multiplied by the  
75 number of reads (Fernandes *et al.*, 2013; Gloor *et al.*, 2016a). Thus, the data returned by HTS are a type  
76 of count compositional data, where only the relationships between the features have meaning (Aitchison,  
77 1986; Lovell *et al.*, 2015; Fernandes *et al.*, 2014; Gloor *et al.*, 2017; Kaul *et al.*, 2017).

78 The ALDEx2 tool uses a combination of probabilistic modelling and compositional data analysis to  
79 determine the features that are different between groups, where that difference is insensitive to random  
80 sampling. Technical replicate variance estimation and conversion of the count data to probabilities is  
81 accomplished by Monte-Carlo sampling from the Dirichlet distribution (Fernandes *et al.*, 2013; Gloor  
82 *et al.*, 2016a), which is conveniently also the conjugate prior for the multivariate Poisson process. The  
83 differences between features is linearized by applying a log-ratio transformation to the Dirichlet Monte-  
84 Carlo realizations and analyzed according to the rules of compositional data analysis (Aitchison, 1986;  
85 Fernandes *et al.*, 2013; Tsilimigras and Fodor, 2016; Gloor *et al.*, 2017).

86 The ‘Group Distribution’ panel in Figure 1 shows the distribution for a gene in a highly replicated  
87 and curated RNA-seq experiment with the expression of the gene in the WT and knockout conditions  
88 shown by the two density distributions. An Anderson-Darling test indicates that a Normal distribution is a  
89 poor fit for both distributions ( $p < 1e - 4$ ). Consequently, standard effect size measures that depend on a  
90 Normality assumption will be expected to perform poorly and the non-parametric method described here

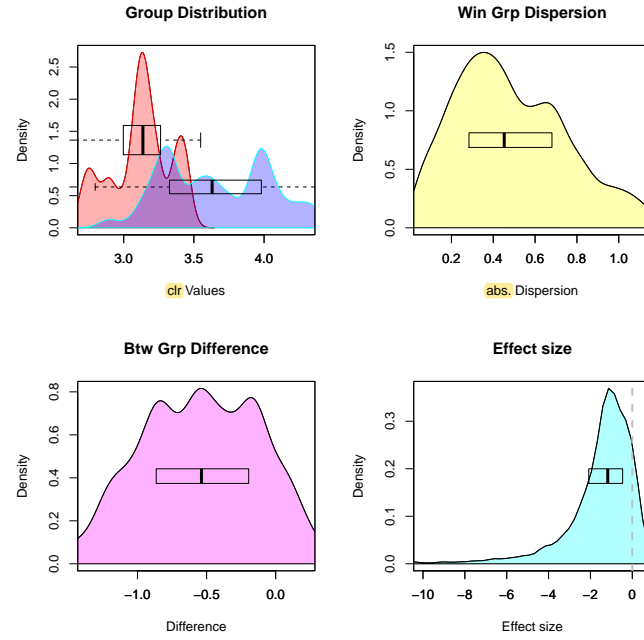


**Figure 1.** The density of read counts may not follow a simple to model distribution. For each distribution the median and interquartile range is shown as the thick vertical line and the enclosing box. The ‘Group Distribution’ panel in the top left shows the density of the read counts in the two groups of a highly replicated RNA-seq experiment conducted in *S. cerevisiae* (Schurch *et al.*, 2016) for the gene YDR171W. We can see that the distributions are partially separated but are strongly multimodal. The ‘Win Grp Dispersion’ shows the density of the within group dispersion of the two groups calculated as outlined in equation 3. The ‘Btw Grp Difference’ shows the density of the between group difference calculated as outlined in equation 2. The ‘Effect size’ shows the density of the effect size calculated as in equation 4. The dashed vertical line in this final panel shows an effect size of 0, and approximately 10% of the effect size distribution crosses this threshold; the proportion of the effect size distribution that crosses an effect of 0 is known as the ‘overlap’ measure.

91 is to be preferred.

92 We will use the distributions for the gene YDR171W in Figure 1 as an example. Starting with  
 93 two vectors  $\vec{a}$  and  $\vec{b}$  that correspond to the concatenated log-ratio transformed Dirichlet Monte-Carlo  
 94 realizations of a feature in two groups, we need a method to determine the standardized effect size; that is,  
 95 the difference between groups relative to an estimate of within-group dispersion. Since these posterior

distributions can have heavy tails, be multimodal, and be skewed, any useful statistic should be insensitive to even extreme non-Normality and provide sensible answers even if the posterior picture distributions are almost Cauchy in one or both groups (Fernandes *et al.*, 2013). Below and in the Supplement we define the properties of the approach used.

We can define a non-parametric *difference* vector in Equation (2) as the signed difference between the two groups

$$\vec{diff} = \vec{a} - \vec{b}, \quad (2)$$

with the distribution of the vector shown in Figure 1 ‘Btw Group Difference’. We can further define a non-parametric *dispersion* vector as in Equation (3), where the notation  $\rho\vec{a}$  indicates one or more random permutations of the vector

$$\vec{disp} = \max\{|\vec{a} - \rho\vec{a}|, |\vec{b} - \rho\vec{b}|\}, \quad (3)$$

with the distribution shown in Figure 1 ‘Win Group Dispersion’. Finally, we can define an *effect* vector as in Equation (4) that is the element-wise ratio of these two vectors

$$\vec{eff} = \frac{\vec{\delta}}{\vec{\sigma}}, \quad (4)$$

with the effect vector shown in Figure 1 ‘Effect size’.

Taking the median of  $\vec{diff}$ ,  $\vec{disp}$  and  $\vec{eff}$  returns a robust estimate of the central tendency of these statistics ( $\tilde{D}$ , MMAD (median of the maximum absolute deviation), and  $\mathbb{E}$ ), and these are the ‘diff.btw’, ‘diff.win’ and ‘effect’ statistics reported by ALDEx2. The location of these summary statistics for each distribution is shown in Figure 1.  $\tilde{D}$  is the very similar to the difference between the means or the difference between medians in a Normal distribution as shown in Supplementary Figure 2. The MMAD metric is novel and the Supplement shows it has a Gaussian efficiency of 52%, a breakdown point of 20% (Supplementary Figure 3), and is 1.42 times the size of the standard deviation on a Normal distribution. The  $\mathbb{E}$  statistic is a standardized effect size and is approximately 0.7 of Cohen’s d when comparing the difference between two Normal distributions. Below and in Supplementary Figure 4 we show that this metric returns sensible values even with a Cauchy distribution.

We used simple simulated datasets to determine baseline characteristics in a number of different distributions. Then we use the data from a highly replicated RNA-seq experiment (Schurch *et al.*, 2016)

113 or from a large 16S rRNA gene sequencing study (Bian *et al.*, 2017) and examined 100 random subsets  
 114 of the data with between 2 and 20 samples in each group. For each random subset we collected the  
 115 set of features that were called as differentially abundant at thresholds of  $\mathbb{E} \geq 1$ , or with an expected  
 116 Benjamini-Hochburg adjusted p-value of  $\leq 0.1$  calculated using either the parametric Welch's t-test, or  
 117 the non-parametric Wilcoxon test in the ALDEx2 R package. These are output as 'we.eBH' and 'wi.eBH'  
 118 by the ALDEx2 tool. These were compared to a 'truth' set determined by identifying those features that  
 119 were identified in all of 100 independent tests of the full dataset with outliers removed using the same  
 120 tests and cutoffs. Note that this is simply a measure of consistency and is congruent with the approach  
 121 taken in (Schurch *et al.*, 2016). We also examined subsets of these datasets where the subsets were taken  
 122 from the same group. This allowed us to characterize the properties of  $\mathbb{E}$  when no difference between  
 123 groups was expected.

## 124 RESULTS AND DISCUSSION

125 The motivation for this work is to identify what features are reliably different even with small sample  
 126 sizes in high throughput sequencing experiments. Measuring differential abundance in high throughput  
 127 sequencing datasets is difficult for a variety of reasons. First, almost all experiments are underpowered.  
 128 Second, the true distribution of the data is unknown. Third, when sample sizes are large almost all features  
 129 are identified as 'significantly different' by null hypothesis significance testing frameworks. This latter  
 130 reason is why guidance is generally to ensure that the feature is below a p-value threshold (or below a q,  
 131 or false discovery rate, threshold and be above a minimum difference threshold (Schurch *et al.*, 2016).

132 We began by examining the behaviour of the  $\mathbb{E}$  metric and its constituent statistics. Supplementary  
 133 Figure 2 shows that the difference between distributions measure is essentially as efficient and stable a  
 134 measure of location as is the difference between means. When comparing measures of scale, Supplemen-  
 135 tary Figure 3 shows that the breakdown point for the MMAD is 20% and the efficiency is approximately  
 136 52% of the standard deviation in a Normal distribution. Thus, the MMAD is reasonably efficient, and  
 137 much less prone to contamination than is the standard deviation. Simulation shows that the MMAD is  
 138 approximately 1.418 larger than the standard deviation for a Normal distribution. Taken together,  $\mathbb{E}$  is  
 139 approximately 0.705 the size of Cohen's d in a Normal distribution, but  $\mathbb{E}$  returns sensible estimates even

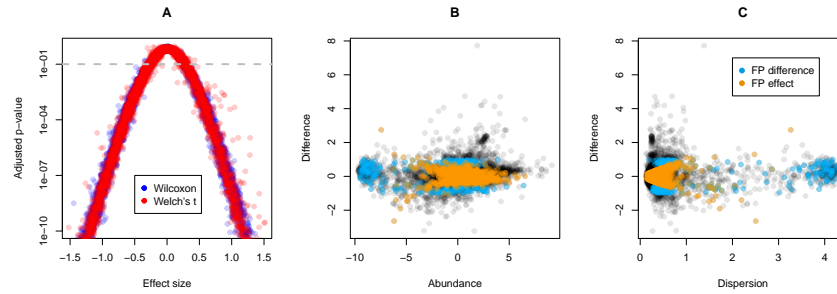


**Figure 2.** Characteristics of false positive features using  $\mathbb{E}$ . Panel A shows the relationship between  $\mathbb{E}$  and Benjamini-Hochberg adjusted p-values calculated by either a non-parametric Wilcoxon test (blue points), or a parametric Welch's t-test (red points), where each point represents one of the genes in the yeast transcriptome dataset. The y axis has been truncated to highlight the p-values greater than  $1e-10$ , and the dashed grey line shows the location of a false positive threshold of 0.1. Panel B shows a Bland-Altman plot of the whole yeast transcriptome dataset in grey points, with the false positive features identified by either difference between groups (blue) or  $\mathbb{E}$  (orange) from identified from a random subset of 5 samples from each group. Panel C shows the same analysis as an effect plot (Gloor *et al.*, 2016b). The false positive features identified by each approach are restricted to features with quite separate characteristics of difference, abundance and dispersion.

140 for non-Normal distributions.

141 With this null behaviour information, we can examine an example dataset of a highly replicated  
 142 RNA-seq dataset generated by (Schurch *et al.*, 2016). In this dataset, the edgeR tool identified over 4600  
 143 out of 6349 genes as 'significant' (Benjamini-Hochberg adjusted p-value  $< 0.05$ ) when all samples were  
 144 included using either the glm or exact test modes (Supplementary Table 1). Other widely used tools gave  
 145 similar results (Schurch *et al.*, 2016). The null hypothesis testing framework in ALDEx2 also returned at  
 146 least 4300 genes in the same dataset. Thus, identifying such a large proportion of genes as differentially  
 147 abundant indicates that statistical significance is not informative for this type of experiment. Schurch *et al.*  
 148 (and others) recommend adding a secondary threshold such as a fold-change cutoff to identify genes of  
 149 interest for follow-up analyses (Cui and Churchill, 2003; Schurch *et al.*, 2016). When sample sizes are  
 150 sufficiently large, we would expect that the fold-change cutoff itself would be the primary determinant of  
 151 difference; however, this approach would not include either the biological variance or the uncertainty of



152 measurement in the analysis.

153 Figure 2: A shows the relationship between  $\mathbb{E}$  and p-value for the 6349 genes in the dataset. We can  
154 see that there is very good correspondence such that features with very high effect sizes have very low  
155 adjusted p-values. This is in line with the expected relationship between effect sizes and p-values, and  
156 provides additional confidence that  $\mathbb{E}$  is an appropriate metric for effect size. However, note that the  
157 non-parametric Wilcoxon test adjusted p-values (in blue) have far fewer outliers on this plot than do the  
158 parametric Welch's t-test adjusted p-values (in red). We conclude that the majority of features likely have  
159 distributions that do not deviate to much from the Normality assumption of the parametric test, but that  
160 there is a significant minority of features that do. These outliers could contribute to both false positive and  
161 false negative identifications when using a parametric null hypothesis testing approach.

162 We next investigated the overlap between false positive features when measured by effect size alone  
163 and when measured by difference alone. This is shown in Figure 2: B and C in two different plots. Here  
164 we can see that false positive features that are identified solely for having a large difference between  
165 groups (at least 2 fold) tend to be made up of features that are very rare and very variable in the dataset.  
166 Conversely, the false-positive features that are identified solely based on  $\mathbb{E} > 1$  tend to be very abundant  
167 and much less variable. We hypothesized that using these two metrics together would show a marked  
168 decrease in false positive identifications, and we tested two methods of combining  $\mathbb{E} > 1$  and difference  
169 between groups to determine which if any was to be preferred.

170 We examined the relationship between sample size and the number of features identified as significantly  
171 different using a null hypothesis testing framework in this dataset and using the effect size and difference  
172 measures. The 'Proportion' plot in Figure 3 shows the median True and False positive rates, and the  
173 'Count' plot in the figure shows the median of the actual count of features identified. Here we are testing  
174 for the ability to detect features that would have been observed as differentially abundant in the full dataset  
175 if we use a random subset of the data, and the plots show the median value of 100 trials at each sample  
176 size. The 'q+diff' example in the Proportion panel shows the rate observed for the Benjamini-Hochberg  
177 corrected p-values (q-values) and a 2-fold difference observed when using the edgeR tool (REF), as  
178 advised in recent best practices (Schurch *et al.*, 2016). As expected we observe that the power of null  
179 hypothesis significance test is strongly affected by sample size, and only reaches 90% power to detect

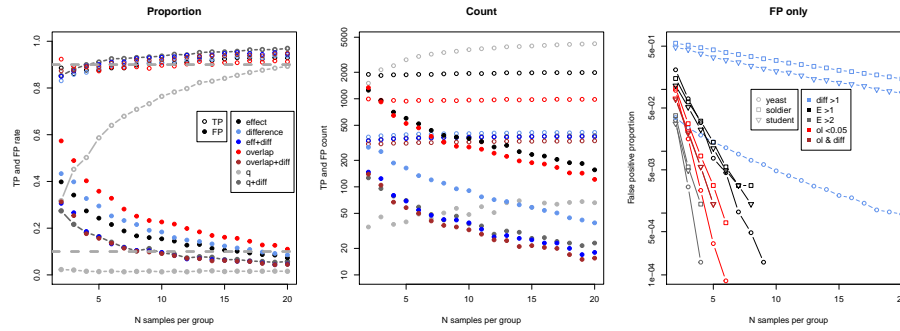


**Figure 3.** True Positive (TP) and False Positive (FP) identifications as a function of per group sample size. The two left panels show the results of sub-sampling the yeast transcriptome dataset. Here the WT and knockout samples were randomly selected 100 times. Features that were identified in the subsample that were identified as different in the full dataset were counted as true positives (TP), and features that were identified in the subsets that were not identified as different in the full dataset were counted as false positives (FP). The proportion panel on the left shows the median proportion of TP found by each approach, and the median proportion of all positives that were FP. The count panel in the middle shows the median feature counts for each approach. Cutoffs used were absolute effect  $\geq 1$ , absolute difference  $\geq 1$ , overlap of  $\geq 0.05$ , or adjusted p-value score of  $\geq 0.1$ . Combination approaches used the intersect of the individual approaches. The FP only panel shows the proportion of all features as a function of per-group sample size in the datasets that were identified as false positive if only one condition was sampled from either the yeast transcriptome, or two different cohorts from a 16S rRNA gene sequencing experiment.

180 when the per-group sample size is greater than 20. Interestingly, applying both the significance test and  
181 the fold-change cutoff reproduced the effect plus fold-change cutoff results nearly exactly in this dataset.  
182 Inspection of the results indicated that this was because in this dataset the significance test was all-but  
183 irrelevant because all features with at least a 2-fold change had a q-score below the threshold of 0.1. Note  
184 that all tools have difficulty estimating the actual FDR in many datasets (Thorsen *et al.*, 2016; Hawinkel  
185 *et al.*, 2018).

186 In contrast to q-scores, the TPR of the  $\mathbb{E}$  statistic in the same random datasets is essentially independent  
187 of the number of samples for all methods and combinations. However, now the FPR is strongly affected  
188 by sample size. Note that even when only two samples are used, the  $\mathbb{E}$  statistic identifies over 80% of  
189 the features as different as are identified by the same statistic in the full dataset. Thus, the simple metric  
190 outlined here can correctly identify the ‘true positive’ set even when the number of samples is very small.  
191 The tradeoff when using this statistic is that at very low sample sizes the False Discovery Rate (fdr) is  
192 extreme; in this dataset and with and with a cutoff of  $\mathbb{E} > 1$ , the fdr is 40% with two samples, but falls to  
193 less than 10% only when there are 15 or more samples. Interestingly, applying a fold-change cutoff to the  
194  $\mathbb{E}$  metric reduces the false discovery rate dramatically and also reduces the number of features identified  
195 as significantly different.

196 The FP only panel of Figure 3 show how many false positive identifications can be expected as a  
197 function of sample size. Here we sub-sampled from one group only in two different datasets; the yeast  
198 transcriptome dataset and two large cohorts from a 16S rRNA gene sequencing dataset (Bian *et al.*, 2017).  
199 We we expect that no features are truly different and plotted the proportion of all features that were  
200 identified as different as a function of per-group sample size. We can see that selecting for a  $\mathbb{E}$  of at least 1,  
201 or an overlap of  $< 0.05$ , rapidly results in no false positive identifications in these subsamples, regardless  
202 of source. In fact, no FP were identified in either dataset with when the  $\mathbb{E} > 1$  when the sample size was  
203 greater than 9, and for the overlap metric when the sample size was greater than 6. Interestingly the decay  
204 curves for FP identification are nearly co-incident for each approach in the two different datasets.

205 Note however, that this investigation highlights the danger in relying on fold-change to identify  
206 differentially abundant features. We can see that the 16S rRNA gene sequencing datasets have substantially  
207 greater numbers of fold-change FP features than does the yeast transcriptome dataset. This is likely

208 because of the substantially greater dispersion observed for the features in the former dataset than in the  
209 latter (supplementary figure x).

## 210 CONCLUSION

211 By default, we want to know both ‘what is significant’ and ‘what is different’ (Cui and Churchill, 2003).  
212 Both of these questions can be addressed with a standardized effect size statistic that scales the difference  
213 between features by their dispersion. We have found plots of difference and dispersion to be an exceeding  
214 useful tool when examining HTS datasets (Gloor *et al.*, 2016b). Furthermore, datasets analyzed by this  
215 approach have proven to be remarkably reproducible as shown by independent lab validation (Macklaim  
216 *et al.*, 2013; Nelson *et al.*, 2015)

217 The  $\mathbb{E}$  statistic outlined here is a relatively robust statistic with the attractive property that it consistently  
218 identifies almost all the same set of true features regardless of the underlying distribution as shown in  
219 Figure 2, and the number of samples as shown in Figure 3. In marked contrast, even the best p-value based  
220 approaches can identify only a small proportion of the features at small samples sizes that would have  
221 been found in the full dataset (Schurch *et al.*, 2016). Thus, the simple metric outlined here can correctly  
222 identify the ‘true positive’ set even when the number of samples is very small. Note that fold-change  
223 thresholds as is commonly used, is not the same as an standardized effect statistic, and applying the  
224 threshold values of (Schurch *et al.*, 2016) while reducing the features that are found does not necessarily  
225 enhance reproducibility (Figure 3: FP only).

226 The tradeoff when using the  $\mathbb{E}$  statistic is that at very low sample sizes the False Discovery Rate can be  
227 extreme; in this dataset and with and with a cutoff of  $\mathbb{E} > 1$ , the FDR is 40% with two samples, but falls  
228 to less than 10% only when there are 15 or more samples. A similar FDR is observed when using only the  
229 overlap measure. However, adding in an absolute fold-change restriction reduces the FDR substantially  
230 and reduces the number of samples needed to reduce the FDR to  $\leq 10\%$  to fewer than 10 samples per  
231 group. Further tempering this, is the observation that no false positives are identified in two different  
232 datasets when there are 10 or more samples per group, and there is no expected difference between groups.  
233 The Supplement shows additional evidence that the  $\mathbb{E}$  statistic is generally useful, having essentially the  
234 same characteristics in a 16S rRNA gene sequencing dataset which has much larger per feature dispersion.

235 Taken together, we suggest that a fold change of at least two, and either  $\mathbb{E} > 1$  or overlap  $\geq 0.05$  are robust  
236 and reproducible measures that provide an acceptable mix of power and specificity when the sample size  
237 is greater than 10 per group.

238 This work describes the  $\mathbb{E}$  statistic that measures a standardized effect size directly from distributions  
239 and not from summary statistics. We show that it is useful when examining high throughput sequencing  
240 datasets. The statistic is relatively robust and efficient, and answers the question most desired by the  
241 biologist, namely ‘what is reproducibly different’.  $\mathbb{E}$  is computed in the ALDEx2 R package as the ‘effect’  
242 output where it is the median of the inferred technical and biological data, and in the distEffect R package  
243 where it acts only the point estimates of the data. Interactive exploration of effect sizes can be done in the  
244 omicplotR Bioconductor package (Giguere *et al.*, 2019).

## 245 ACKNOWLEDGEMENTS

246 To be determined

## 247 FUNDING

248 This work has been supported by NSERC, CIHR.

## 249 REFERENCES

- 250 Aitchison, J. (1986). *The Statistical Analysis of Compositional Data*. Chapman & Hall.
- 251 Bian, G., Gloor, G. B., Gong, A., Jia, C., Zhang, W., Hu, J., Zhang, H., Zhang, Y., Zhou, Z., Zhang, J.,  
252 Burton, J. P., Reid, G., Xiao, Y., Zeng, Q., Yang, K., and Li, J. (2017). The gut microbiota of healthy  
253 aged chinese is similar to that of the healthy young. *mSphere*, **2**(5), e00327–17.
- 254 Coe, R. (2002). It’s the effect size, stupid: What effect size is and why it is important.
- 255 Colquhoun, D. (2014). An investigation of the false discovery rate and the misinterpretation of p-values.  
256 *R Soc Open Sci*, **1**(3), 140216.
- 257 Cui, X. and Churchill, G. A. (2003). Statistical tests for differential expression in cdna microarray  
258 experiments. *Genome Biol*, **4**(4), 210.1 – 210.10.
- 259 Cumming, G. (2008). Replication and p intervals: p values predict the future only vaguely, but confidence  
260 intervals do much better. *Perspect Psychol Sci*, **3**(4), 286–300.

261 Fernandes, A. D., Macklaim, J. M., Linn, T. G., Reid, G., and Gloor, G. B. (2013). Anova-like differential  
 262 expression (aldex) analysis for mixed population rna-seq. *PLoS One*, **8**(7), e67019.

263 Fernandes, A. D., Reid, J. N., Macklaim, J. M., McMurrough, T. A., Edgell, D. R., and Gloor, G. B.  
 264 (2014). Unifying the analysis of high-throughput sequencing datasets: characterizing RNA-seq, 16S  
 265 rRNA gene sequencing and selective growth experiments by compositional data analysis. *Microbiome*,  
 266 **2**, 15.1–15.13.

267 Giguere, D., Macklaim, J., and Gloor, G. (2019). omicplotr: Visual exploration of omic datasets using a  
 268 shiny app. Bioconductor v1.4.0.

269 Gloor, G. B., Macklaim, J. M., Vu, M., and Fernandes, A. D. (2016a). Compositional uncertainty should  
 270 not be ignored in high-throughput sequencing data analysis. *Austrian Journal of Statistics*, **45**, 73–87.

271 Gloor, G. B., Macklaim, J. M., and Fernandes, A. D. (2016b). Displaying variation in large datasets:  
 272 Plotting a visual summary of effect sizes. *Journal of Computational and Graphical Statistics*, **25**(3C),  
 273 971–979.

274 Gloor, G. B., Macklaim, J. M., Pawlowsky-Glahn, V., and Egozcue, J. J. (2017). Microbiome datasets are  
 275 compositional: And this is not optional. *Front Microbiol*, **8**, 2224.

276 Halsey, L. G., Curran-Everett, D., Vowler, S. L., and Drummond, G. B. (2015). The fickle p value  
 277 generates irreproducible results. *Nat Methods*, **12**(3), 179–85.

278 Hawinkel, S., Mattiello, F., Bijmens, L., and Thas, O. (2018). A broken promise : microbiome differential  
 279 abundance methods do not control the false discovery rate. *BRIEFINGS IN BIOINFORMATICS*.

280 Ioannidis, J. P. A. (2005). Why most published research findings are false. *PLoS Med*, **2**(8), e124.

281 Kaul, A., Mandal, S., Davidov, O., and Peddada, S. D. (2017). Analysis of microbiome data in the  
 282 presence of excess zeros. *Front Microbiol*, **8**, 2114.

283 Lovell, D., Pawlowsky-Glahn, V., Egozcue, J. J., Marguerat, S., and Bähler, J. (2015). Proportionality: a  
 284 valid alternative to correlation for relative data. *PLoS Comput Biol*, **11**(3), e1004075.

285 Macklaim, J. M., Fernandes, A. D., Di Bella, J. M., Hammond, J.-A., Reid, G., and Gloor, G. B. (2013).  
 286 Comparative meta-rna-seq of the vaginal microbiota and differential expression by lactobacillus iners  
 287 in health and dysbiosis. *Microbiome*, **1**(1), 12.

288 Nakagawa, S. (2004). A farewell to bonferroni: the problems of low statistical power and publication

289 bias. *Behavioral Ecology*, **15**(6), 1044–1045.

290 Nelson, T. M., Borgogna, J.-L. C., Brotman, R. M., Ravel, J., Walk, S. T., and Yeoman, C. J. (2015).

291 Vaginal biogenic amines: biomarkers of bacterial vaginosis or precursors to vaginal dysbiosis? *Frontiers*

292 *in physiology*, **6**.

293 Schurch, N. J., Schofield, P., Gierliński, M., Cole, C., Sherstnev, A., Singh, V., Wrobel, N., Gharbi,

294 K., Simpson, G. G., Owen-Hughes, T., Blaxter, M., and Barton, G. J. (2016). How many biological

295 replicates are needed in an rna-seq experiment and which differential expression tool should you use?

296 *RNA*, **22**(6), 839–51.

297 Sonesson, C. and Delorenzi, M. (2013). A comparison of methods for differential expression analysis of

298 RNA-seq data. *BMC Bioinformatics*, **14**, 91.

299 Thorsen, J., Brejnrod, A., Mortensen, M., Rasmussen, M. A., Stokholm, J., Al-Soud, W. A., Sørensen,

300 S., Bisgaard, H., and Waage, J. (2016). Large-scale benchmarking reveals false discoveries and count

301 transformation sensitivity in 16S rRNA gene amplicon data analysis methods used in microbiome

302 studies. *Microbiome*, **4**(1), 62.

303 Tsilimigras, M. C. B. and Fodor, A. A. (2016). Compositional data analysis of the microbiome: funda-

304 mentals, tools, and challenges. *Ann Epidemiol*, **26**(5), 330–5.

305 E Weiss, S., Xu, Z. Z., Peddada, S., Amir, A., Bittinger, K., Gonzalez, A., Lozupone, C., Zaneveld, J. R.,

306 Vázquez-Baeza, Y., Birmingham, A., Hyde, E. R., and Knight, R. (2017). Normalization and microbial

307 differential abundance strategies depend upon data characteristics. *Microbiome*, **5**(1), 27.